

A New Class of Biodegradable Materials: Poly-3-hydroxybutyrate/Steam Exploded Straw Fiber Composites.

I. Thermal and Impact Behaviour

MAURIZIO AVELLA,¹ EZIO MARTUSCELLI,^{*1} BENIAMINO PASCUCCI,¹ MARIA RAIMO,¹ BONAVENTURA FOCHER,² and ANNAMARIA MARZETTI²

¹Istituto di Ricerche su Tecnologia dei Polimeri e Reologia del C.N.R., Via Toiano, 6-80072 Arco felice, Napoli, Italy, Consorzio sulle Applicazioni dei Materiali Plastici e per i problemi di Difesa dalla Corrosione, Via P. Castellino, 111 80100, Napoli, Italy, and ²Stazione Sperimentale per la Cellulosa, Carta e Fibre Tessili Vegetali ed Artificiali, Piazza Leonardo da Vinci, 26-20133 Milano, Italy

SYNOPSIS

Biodegradable thermoplastic composites reinforced with wheat straw fibers were prepared. The matrix was an expensive polyester, poly-3-hydroxybutyrate (PHB), produced by bacterial fermentation. Before being mixed with the PHB, the wheat straw fibers were subjected to a steam explosion process that induces morphological and structural changes in lignocellulosics. Such changes enhance the interaction with the thermoplastic matrix. The two components were melt mixed and the composite molded under hot compression. Compared with neat PHB, not only does the composite material show better mechanical properties but, moreover, production costs are dramatically reduced because wheat straw is a very inexpensive product. Finally, FTIR measurements revealed some PHB/straw fiber molecular interactions that interfere with the PHB crystallization. © 1993 John Wiley & Sons, Inc.

INTRODUCTION

During recent years there has been an increasing demand for new materials with tailored technological properties like low density, high modulus, high strength, and toughness. Furthermore the need to contain environmental pollution makes biodegradability essential in today's materials. Multicomponent polymeric systems like polymer blends and composites have, in many cases, met the target, mainly in terms of their physico-mechanical performance and their relatively low production costs.

Intermolecular interactions between polymers are key factors in governing the strength and stability of composite interfaces. Cellulose fibers are very effective in forming intermolecular hydrogen bonds with thermoplastic polymers, hence producing low density, high modulus/high strength composites.^{1,2} However the wall cellulose in wood cells is associated

with hemicelluloses and lignin, two polymers that from the morphological and structural points of view are considered as nonfibrous amorphous polymers. Thus the attainment of high performance multicomponent polymeric systems by lignocellulosics rests mainly on two factors:

1. fractionation of lignocellulosics into their components to obtain either neat cellulose, or cellulose associated with a small quantity (5–10%) of hemicelluloses and lignin;
2. changes in the morphology and structure of the lignocellulosic components to enhance their faculty to form interfacial bonds with thermoplastic polymers.

The fractionation of lignocellulosics can be achieved by chemical or mechanical treatment; in recent years a new process, called the steam explosion process (SEP), has been proposed.^{3–6} This process not only leads to highly fractionated lignocellulosic materials but also increases the reactivity of the materials themselves.

* To whom correspondence should be addressed.

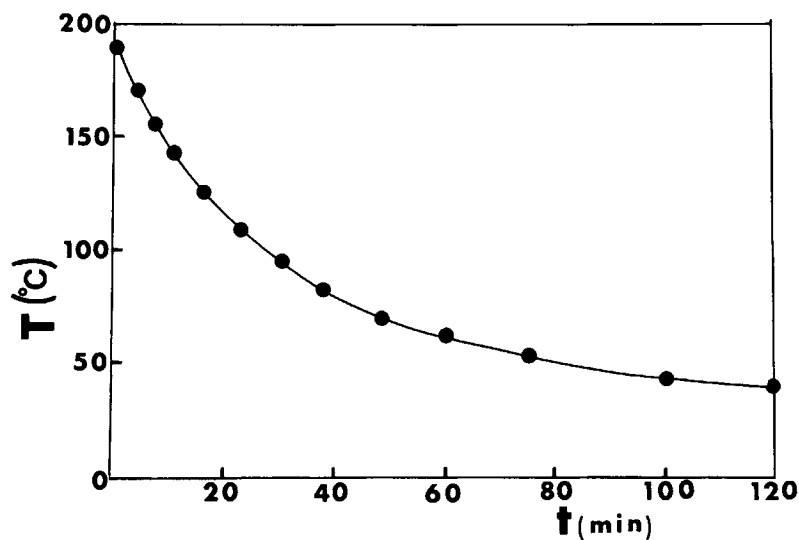


Figure 1 Experimental curve of cooling rate used to prepare the samples by compression molding.

The aim of the present work was to use inexpensive steam exploded straw fibers to prepare composites with a matrix of a biodegradable microbial

polyester like PHB.⁷ PHB is a crystalline thermoplastic polymer that has a well-defined melting point, and properties similar to those of conventional



Figure 2 Optical micrographs of straw fibers after SEP: (A) $T = 205^{\circ}\text{C}$, $t = 2$ min; (B) $T = 220^{\circ}\text{C}$, $t = 2$ min; (C) $T = 235^{\circ}\text{C}$, $t = 2$ min.

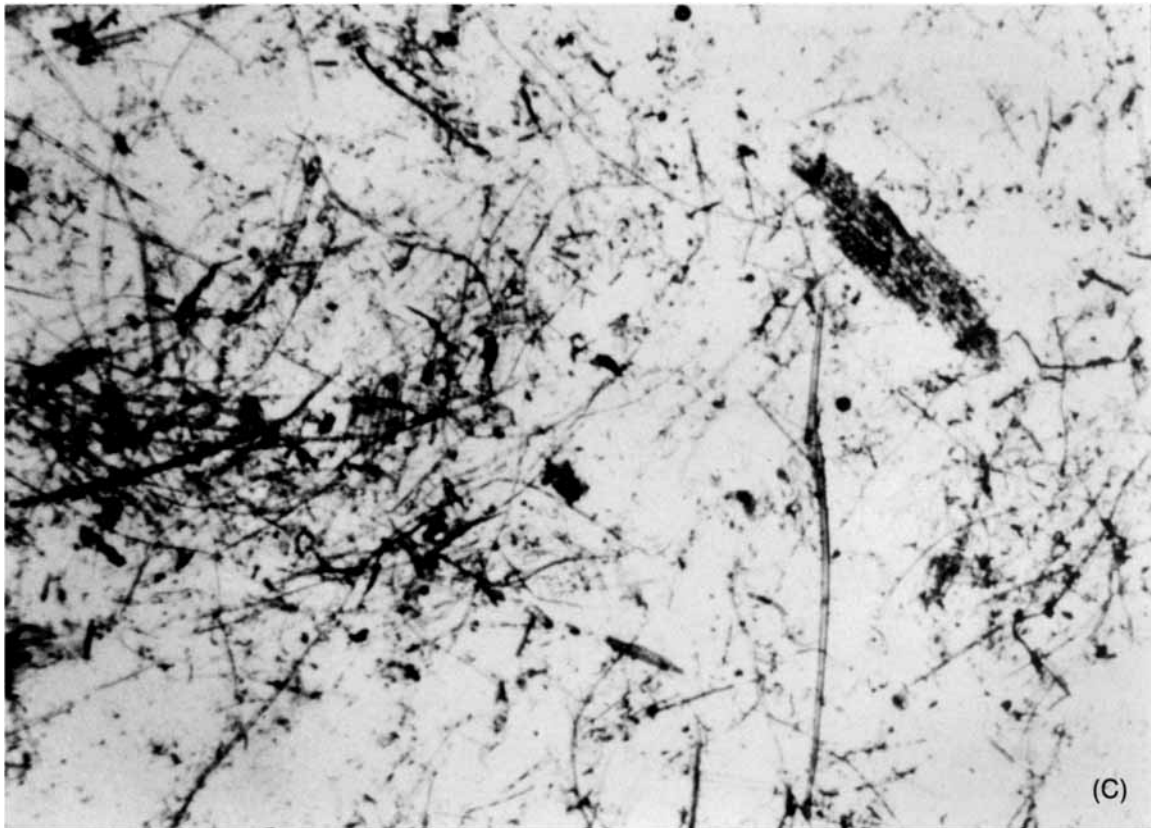


Figure 2 (Continued from the previous page)

polyesters. It has attracted industrial interest as a possible candidate for large-scale biotechnological products, but until now has had limited industrial application because of its high cost and relatively low resistance to impact.⁸

EXPERIMENTAL

Materials and Preparation of Composites

PHB, molecular weight, MW = 400,000, was supplied by ICI and used as received. The wheat straw (Italian and EC sources), 100 g per sample, was steam exploded in laboratory apparatus (Deltalab EC 300) as follows: The straw was put into the vessel and heated with saturated vapor at 230°C (28 kgf/cm²) for a residence time of 120 s. At the end of this time the sudden release of pressure leads to an adiabatic expansion of the water present in the wood tissues. The straw fibers were discharged into the cyclon receiver, collected and placed in an oven (80°C) for a period of time sufficient to release the water adsorbed during the steam explosion process, after which the straw was packed in polyethylene bags and frozen for storage. When the time came to prepare the composites, the straw fibers were blended with the PHB for 5 min in a Brabender-like apparatus, operating at 180°C with a roller speed of 32 rotations per minute. Earlier analyses had already established that under such processing conditions no appreciable thermomechanical degradative effects, especially for PHB, took place.⁹ The resultant material was dipped into liquid nitrogen, ground in a mill, and the ground mass completely dried in an oven at 80°C; the dry composite was then compression molded at 180°C for 7 min at $p = p_{atm}$ and then at 180°C for 1 min at $p = 15$ MPa. The molded composite was cooled quickly according to the curve reported in Figure 1.

Using the same conditions an attempt was made to blend PHB with untreated straw (not steam exploded); the resulting material lacked compactness because there were no cohesive forces between the two components.

Methods

X-Ray Diffractometry

The x-ray powder patterns were recorded using Ni-filtered CuK α radiation from a Siemens 500 D Diffractometer equipped with a scintillator counter and a linear amplifier.

FT-IR Spectroscopy

The infrared spectra were obtained with a Bruker IFS 66 FT-IR spectrometer, using KBr pellets for the solid samples¹⁰ and deuterated chloroform for the samples solutions (2%, w/v). The reproducibility of the spectra was verified on two preparations of ground samples. The ground mixture was dried at 70°C under vacuum for 16 h before pressing. Between 16 and 100 scans were taken with a resolution of 4 cm⁻¹.

In order to visualize details in the band shape and the unresolved band components, the Fourier self-deconvolution (FDS) procedure was applied using Bruker software with the methods of Kauppinen et al.¹¹ Unresolved bands became apparent if the band separation was greater than the instrumental resolution. To avoid side lobes and preserve the constancy of the sample band areas, the values chosen for the half-width Lorentzian line and the resolution

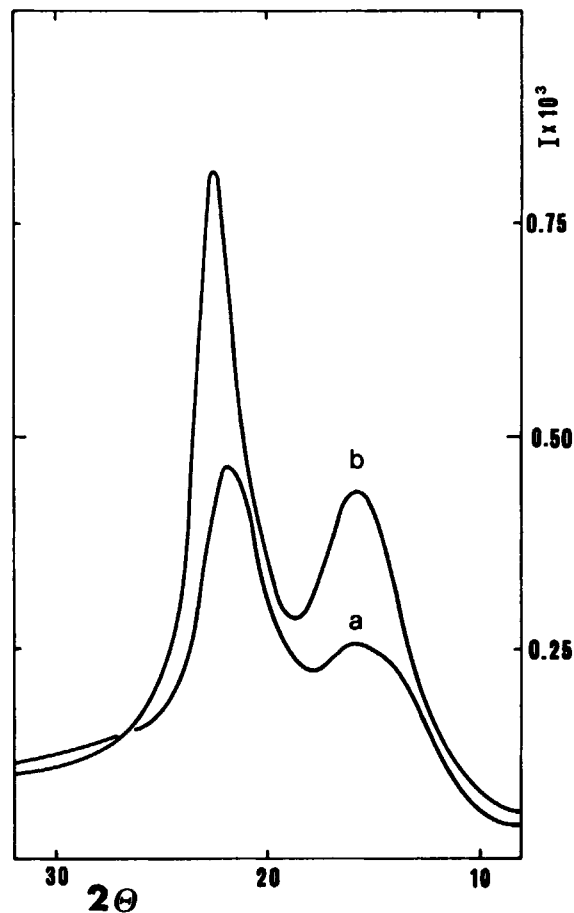


Figure 3 X-ray diffraction patterns of wheat straw: (a) untreated (b) treated at 230°C for 2 min.

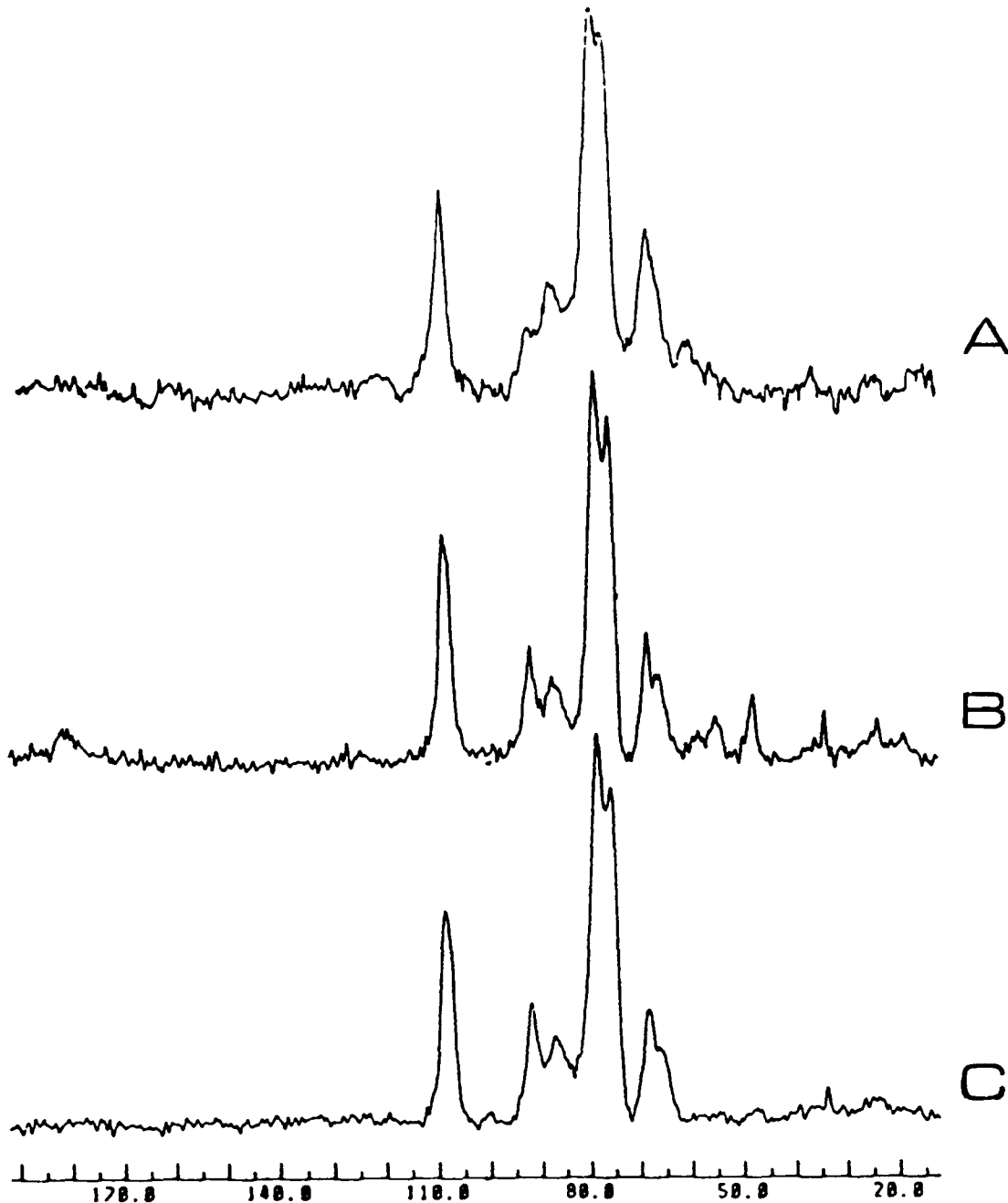


Figure 4 CP-MAS¹³C-NMR spectra of wheat straw: (A) untreated; (B) treated at 230°C for 2 min and extracted with H₂O and 0.5 N NaOH; (C) treated at 230°C for 2 min and extracted with dioxane : water (80 : 20).

enhancement factor were, respectively, 13–15 and 1.3 cm⁻¹.¹¹

The signal-to-noise ratio was better than 500 and the best quantitative information was obtained from the fitting of deconvoluted spectra^{12,13} using Fit, a Fortran program in Bruker software using an interactive procedure.

CP-MAS¹³C-NMR Spectroscopy

The CP-MAS¹³C-NMR spectra were obtained with a Bruker CXP-300 (75 MHz) spectrometer. The cross-polarization time was 1 ms, while the repetition time and the ¹H 90° pulse were 10 s and 3.5 μs, respectively. The full width at half-height of the ref-

Table I Thermal Parameters of PHB/Straw Composites

Parameter	PHB Neat	PHB/Straw 90/10	PHB/Straw 80/20	PHB/Straw 70/30	PHB/Straw 50/50
T_m (°C)	173	170	170	167	167
X_c (%)	57	57	55	57	53
T_c (°C)	91	86	85	82	81
X_c (%)	43	44	42	46	45
T_{m1} (°C)	163	162	161	159	158
T_{m2} (°C)	171	170	170	169	169
X_c (%)	53	53	53	56	54
T_g (°C)	2	4	4	10	ND

ND, not determined.

erence glycine was 27 MHz. Chemical shifts were measured with respect to trimethylpropionic acid sodium salt (TSP); 500–3000 scans were taken; rotational speed was about 3.4 KHz.

DSC Analysis

Thermal investigations were carried out with a Mettler TA-3000 apparatus equipped with a control and programming unit (microprocessor TC-11) and a calorimetric cell. To thermally characterize the materials the samples were heated from 30°C to 200°C (I run). The melting temperature and crystallinity were determined from DSC endotherms. The crystallinity content was calculated by the relation $X_c = \Delta H^* / \Delta H$, ΔH^* being the apparent enthalpy of melting per gram of PHB in the composite, and ΔH the heat required to melt 1 g of neat crystalline PHB ($\Delta H_{PHB} = 146 \text{ J/g}^8$; after 2 min at

200°C the samples were cooled down to 30°C (II run) and the crystallization exotherms and crystallization temperature registered. In the final step the samples were reheated up to 200°C (III run) and the melting point and crystallinity again measured. A scan rate of 10°C/min was used throughout.

The glass-transition temperature (T_g) was ob-

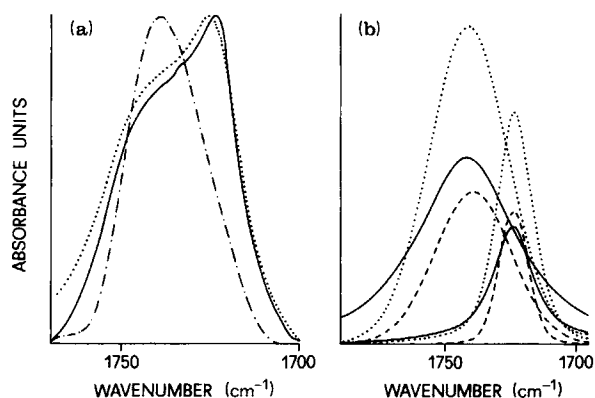


Figure 5 FTIR spectra in the 1800–1700 cm^{-1} region: (a) deconvoluted spectra: (· · · ·) PHB solution; (· · · ·) PHB heated at 160°C, 20 min; (— — —) PHB/straw 50% (w/w); (b) curve fit of: (· · · ·) PHB heated at 160°C, 20 min; (— — —) PHB/straw 30% (w/w); (— — —) PHB/straw 50% (w/w).

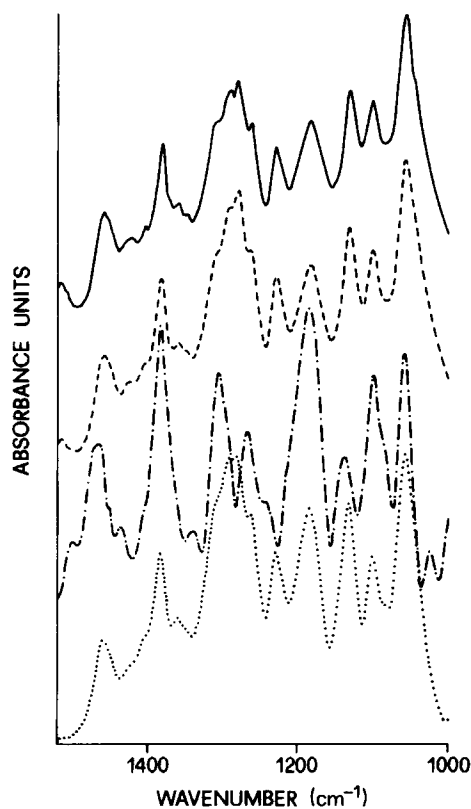


Figure 6 FTIR spectra in the 1500–1000 cm^{-1} region (— — —) PHB/straw 50% (w/w); (— — —) PHB/straw 30% (w/w); (· · · ·) PHB solution; (· · · ·) PHB heated at 160°C, 20 min.

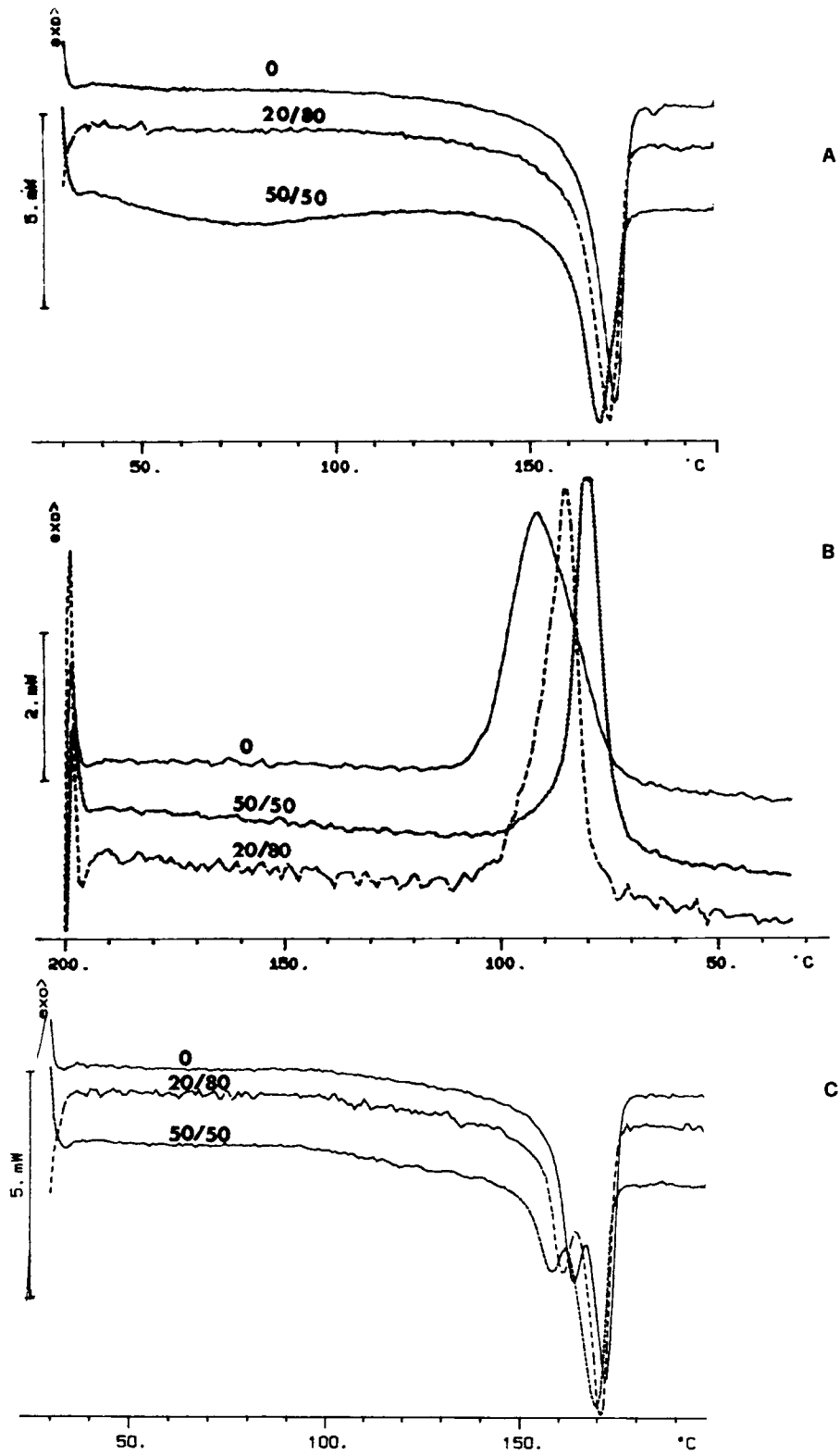


Figure 7 DSC traces of PHB/SE straw composites: (A) I run; (B) nonisothermal crystallization; (C) II run.

Table II Fracture Parameters of PHB/Straw Composites

Parameter	PHB Neat	PHB/Straw 90/10	PHB/Straw 80/20	PHB/Straw 70/30	PHB/Straw 50/50
K_c	1.8	2.2	2.2	1.8	1.6
G_c	1.1	1.4	1.3	1.1	1.1

tained by heating samples that had first been melted at 200°C and then rapidly quenched at -50°C.

Impact Tests

Charpy impact tests were performed with an Instrumented Pendulum (Ceast Autographic Pendulum MK2) on samples 6.0 × 60 mm in dimension, cut by a mill from 3.5-mm thick sheets obtained by hot compression molding. The specimens were notched at the middle of their length as follows: first a blunt notch was made with a v-shaped machine tool and then a sharp notch 0.2-mm deep was produced by a razor blade fixed on a micrometric apparatus. After fracturing the sample the final notch depth value was measured using an optical microscope. The Charpy impact tests were carried out at room temperature at an impact speed of 1 m/s ac-

cording to ASTM-D256 Standards; for each composite six specimens were broken.

Scanning Electron Microscopy Analysis

A Philips 501 scanning electron microscope (SEM) was used to analyze the fracture surfaces after impact breakage. Prior to the analysis the samples were metallized with a Au/Pd alloy, by means of a Polaron Sputtering apparatus.

RESULTS AND DISCUSSION

Steam Explosion Process of Wheat Straw

The morphology and structure of wheat straw undergo marked changes after SEP. In fact, the release of pressure induces an extensive fractionation

Fracture parameters of PHB/straw system

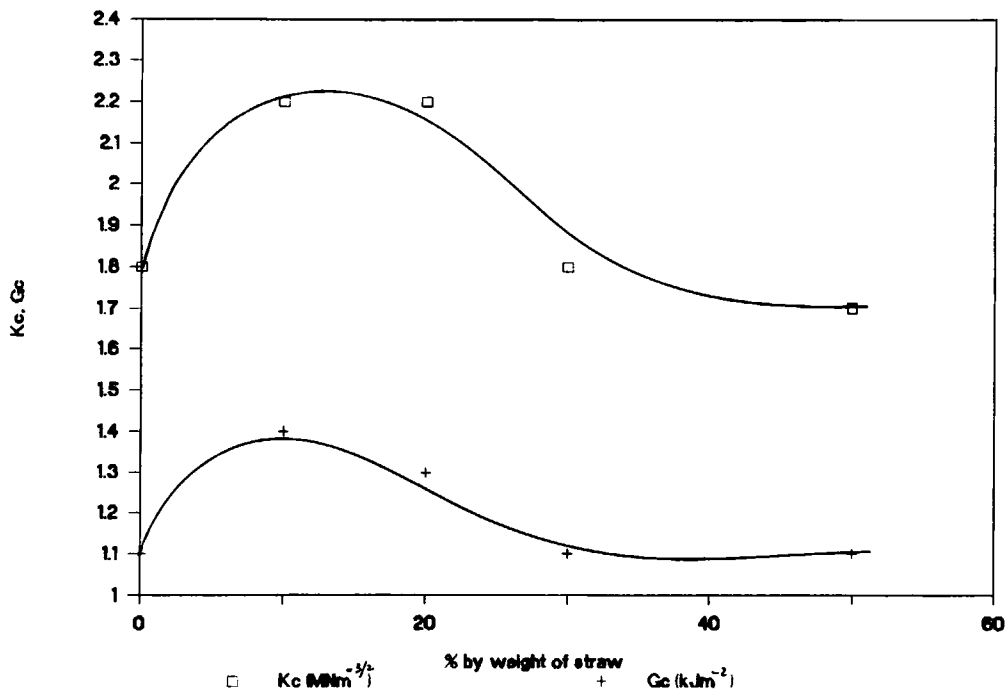
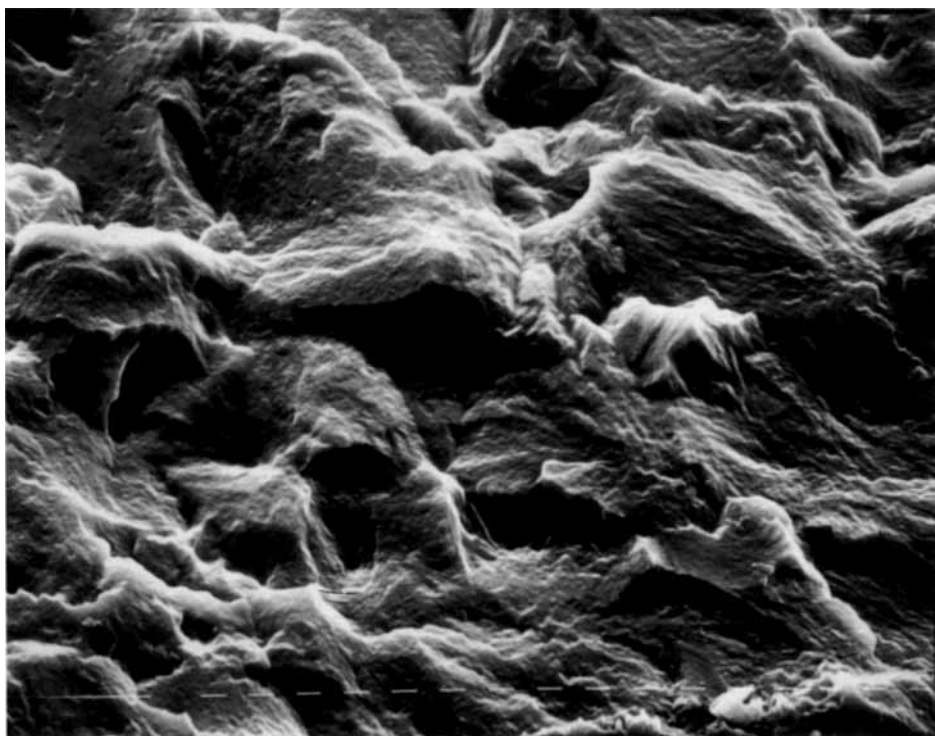
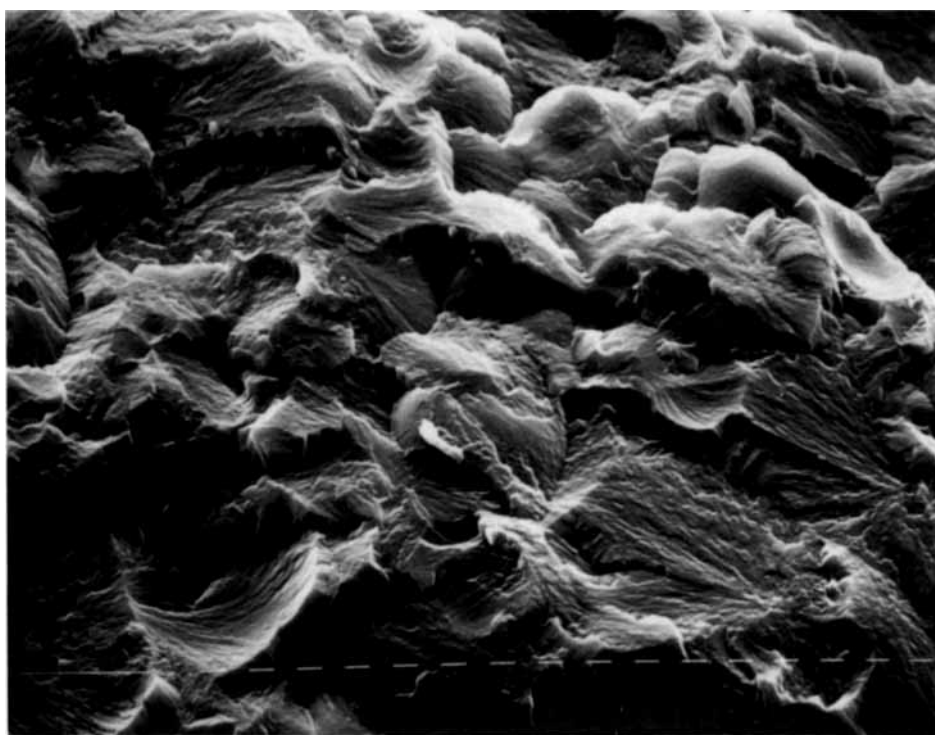


Figure 8 Fracture parameters (K_c and G_c) against percent straw fiber content (w/w).



(a)

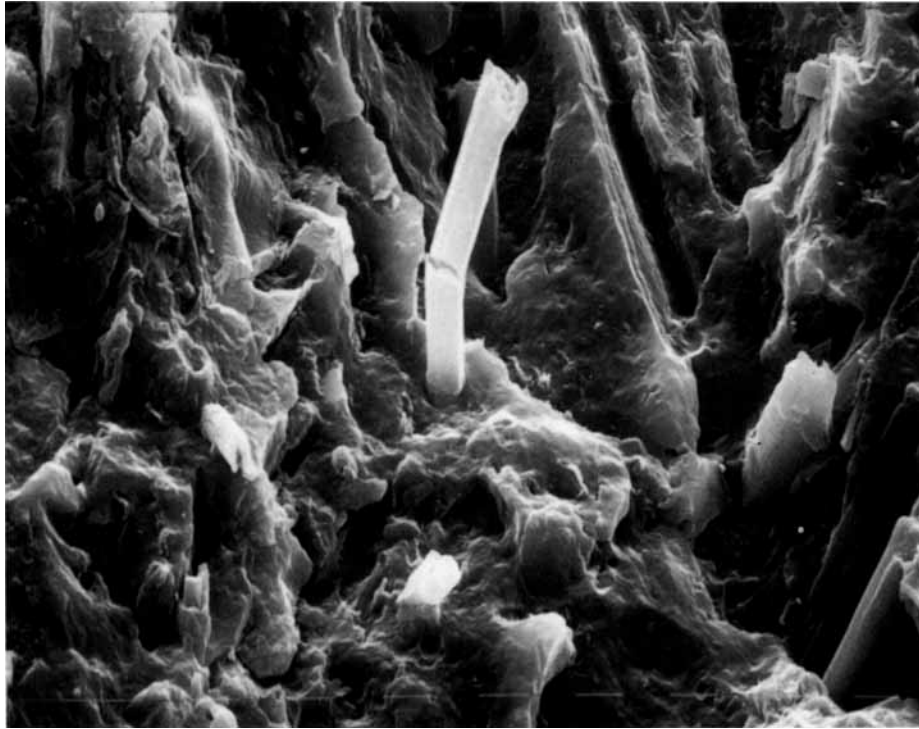


(b)

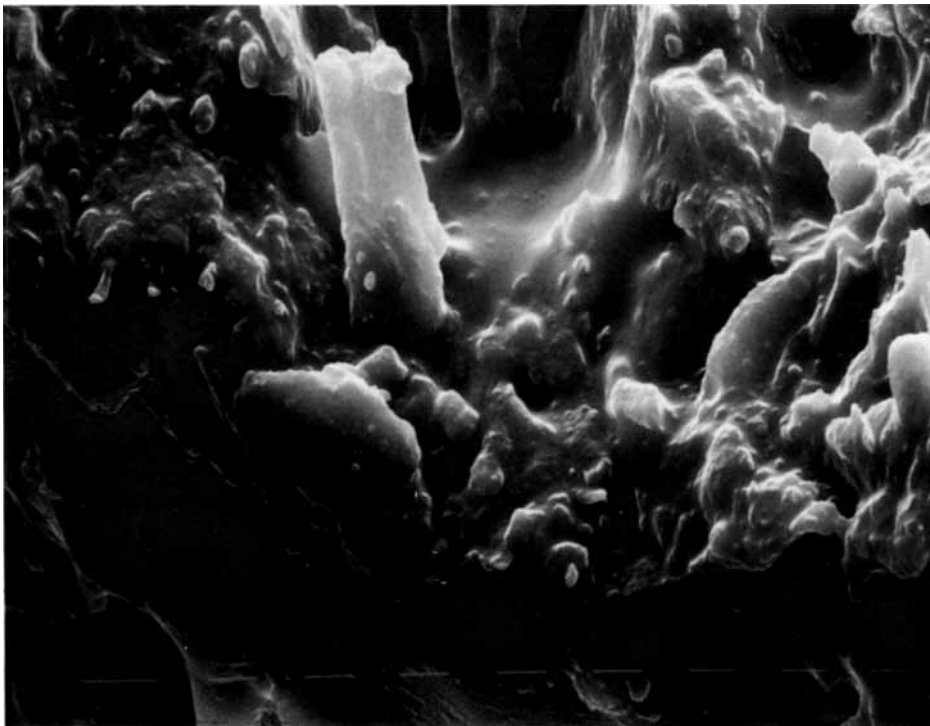
Figure 9 Scanning electron micrographs of fracture surface of neat PHB: (a) 160 \times ; (b) 320 \times .

of the solid matrix, and an autohydrolysis reaction induces a large reduction of the lignin and hemicellulose content, without markedly depolymerizing the

cellulose chains.³⁻⁶ It was observed that at low pressure and short reaction times a gradual defibrillation of material took place, the vessels and epidermal



(a)

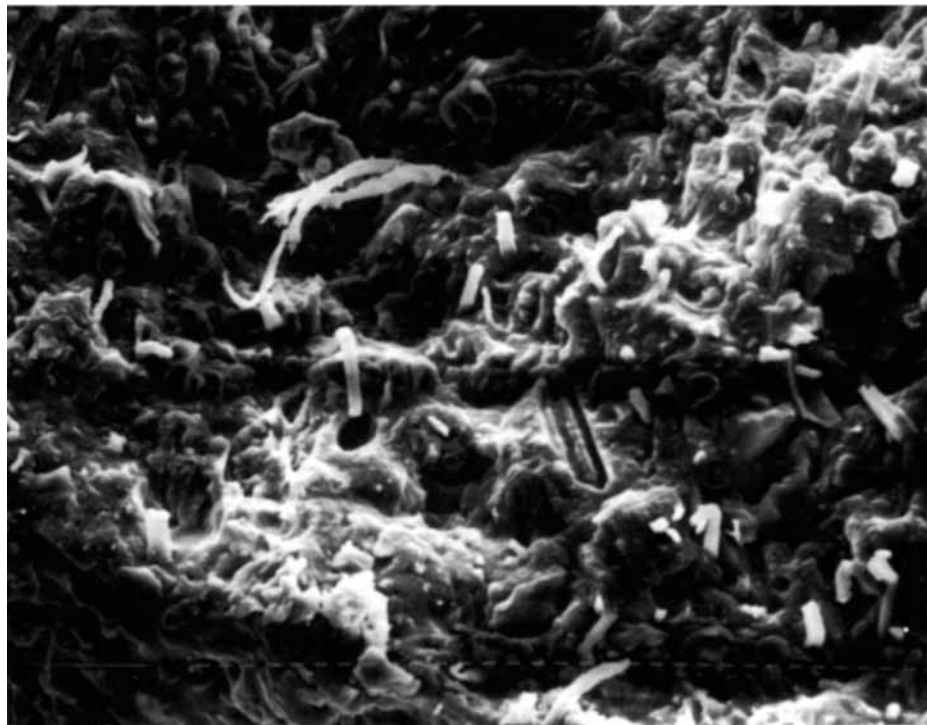


(b)

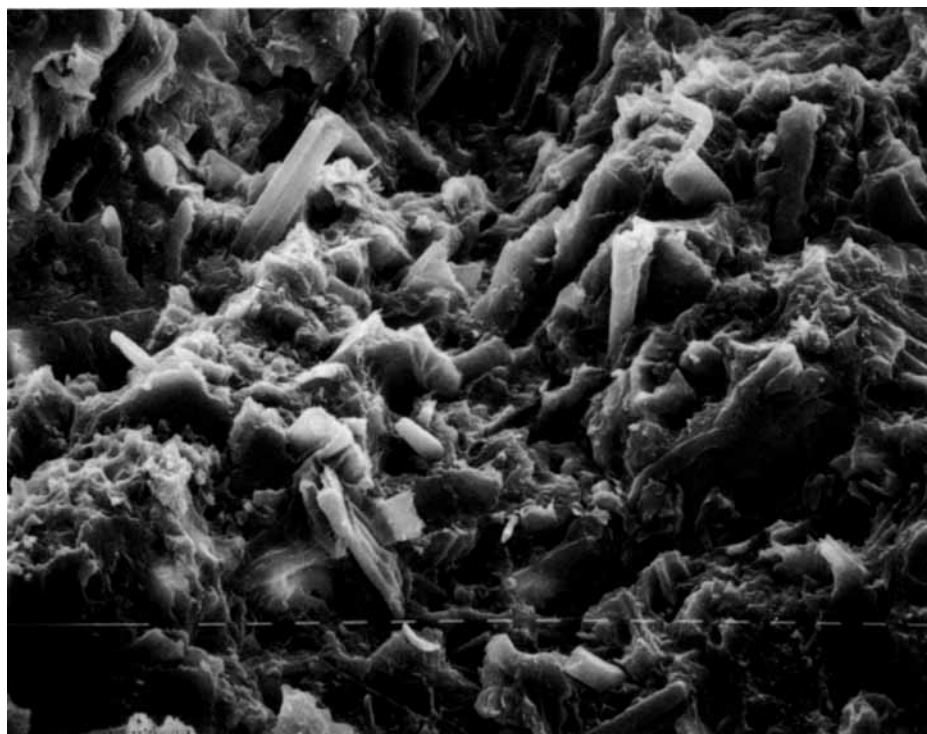
Figure 10 Scanning electron micrographs of fracture surface of PHB/straw composites: (a) 90/10% (w/w); 640X; (b) 80/20% (w/w), 640X; (c) 70/30% (w/w), 160X; (d) 50/50% (w/w), 320X.

tissues of the straw being almost completely destroyed [Fig. 2 (a,b,c)]. Under more severe conditions the straw was mostly defibrillated to single

shorter fibers and brown oily substances were detected, probably arising from lignin and/or extractives condensation. Furthermore, evaluations of the



(c)



(d)

Figure 10 (Continued from the previous page)

surface area of the SE straw showed a marked increase on passing from the untreated sample to the differently treated samples.

After SEP the X-ray diffractograms (Fig. 3) show an increase in the crystallinity degree of the straw

cellulose as well as an increase in the crystal dimension, as evidenced by the sharpening of the reflection related to the (002) crystallographic plan.

An increase of ordered regions in the straw cellulose was also revealed by the sharpening of the

cellulose signals in the CP-MAS ^{13}C -NMR spectra (Fig. 4), as well as by changes in the profile of some signals (C-4, C-6), suggesting a crystallization of the less ordered cellulose during the SEP, similar to that occurring in the annealing treatments of synthetic polymers.

Thus SEP destroys the morphology of natural straw, eliminates most lignin and hemicellulose components, and increases the anisotropy of cellulose fibers, permitting the use of these fibers as reinforcing fibers with a high capacity to interact with thermoplastic polymers.

FTIR Investigations

FTIR were investigated in the regions of both C—H stretching ($3100\text{--}2700\text{ cm}^{-1}$) and deformations ($1500\text{--}1000\text{ cm}^{-1}$), as well as in the region of the carbonyl groups ($1780\text{--}1700\text{ cm}^{-1}$). The bands of PHB/straw composite stretching showed a slightly more detailed structure than that of the neat PHB (heated under the same conditions, 160°C , 20 min) used for the preparation of the PHB/straw composites. As expected marked differences were observed in the spectrum of the PHB solution; in fact most bands evident in the spectrum of the solid samples were not observed, though a more intense band at 2900 cm^{-1} , peculiar to the isotropic state of PHB, occurred.

In the C=O stretching region [Fig. 5(a)] both the neat PHB and the composite show two populations of C=O groups not observed in the spectrum of the PHB solution. By applying a fitting procedure [Fig. 5(b)] the C=O band of the solid samples was split into two bands at 1740 and 1724 cm^{-1} . The lower frequency band seems to be related to the C=O population involved in the crystalline zones: the higher the straw content in the composites the lower the intensity of this band. According to the DSC investigation, this fact seems to suggest that the straw interferes with the PHB crystallization through some intermolecular interactions between the straw hydroxyl groups and the PHB C=O groups.

In the region sensitive to the variation of crystallinity, the neat PHB shows three bands at 1279 , 1228 , and 1185 cm^{-1} , the first being a composite band (Fig. 6). As observed by Marchessault et al.,⁴ the intensity of the band at 1279 cm^{-1} increases by increasing the extent of the ordered region, hence it is higher for neat PHB than for the PHB/straw composites at different straw content. Less significant differences were found for the band at 1185 cm^{-1} , this band⁴ being representative of the PHB amorphous state.

Thermal Investigation

Table I and Figure 7, respectively, show the thermal data and the thermograms obtained using DSC.

The DSC thermograms of PHB and PHB/straw composites show an endothermic double peak when heated from room temperature to 200°C (I run). The melting temperature slightly decreases with the increase in the straw content, but the crystallinity content seems to be almost constant. The DSC traces obtained during the nonisothermal crystallization (II run) show only one exothermic peak. The values of the maximum (T_c) seem to decrease with respect to neat PHB. This finding can be related to the fact that the formation of the straw/PHB interactions, evidenced by FTIR measurements, may delay the crystallization process. Thermograms of the III run show an endothermic double peak for both composites and neat PHB, probably caused by a recrystallization phenomenon that occurs simultaneously with the melting process. Thus the overall thermal effect is the result of two contributions: one the endothermic, corresponding to the melting of the crystals, and the other exothermic, caused by the crystallization of the undercooling melt in aggregates of greater perfection.¹⁵

In the composite materials the T_g values of PHB show, with respect to neat PHB, a slight increase, suggesting that the interactions between the PHB and straw are mainly confined to the nonordered regions.

Impact Behavior and Fractographic Analysis

Table II and Figure 8, respectively, report for all the examined samples the critical strain energy release rate, G_c , and the critical stress intensity factor, K_c , calculated according to the Linear Elastic Fracture Mechanics (LEFM) theory as a function of straw fiber content.^{16–18}

The K_c and G_c values of composite materials containing 10 or 20% straw fiber are higher than those of neat PHB, while composite materials containing 30 and 50% straw fiber present about the same values as neat PHB. This indicates that the fiber plays an important role toward the reinforcement of PHB, probably because of the high adhesion between fibers and matrix. In fact if adhesion is good a high load is necessary to cause separation of the matrix at the interface where the stress concentration is maximum.

The result on the fracture behavior can be interpreted on the basis of fractographic analyses performed by SEM on the fractured surface of notched

specimens. The SEM micrographs were taken near the notch tip in the region of crack initiation.

The fracture surface of neat PHB shows features of a very brittle material [Fig. 9 (a,b)]. No evidence of the formation of crazes and/or shear bands is observed.

Figure 10(a–d) shows SEM micrographs of the PHB–straw composite material. These micrographs show a fine distribution of straw fibers in the PHB matrix, a very high interaction at the fiber–matrix interface, and the presence of some plastic deformation phenomena in the regions adjacent to the fibers.

Comparison of the G_c and K_c values make it evident that 10% and 20% straw seem to be an optimum content for toughening PHB. In fact any further increase in the straw content results in a decrease in the G_c and K_c values to those of the PHB homopolymer.

CONCLUSIONS

PHB/straw composites represent a new class of biodegradable materials that, considering their performance and the reduction of PHB costs, have great industrial potential.

The addition of 10–20% steam exploded straw to PHB markedly increases the physico–mechanical characteristics of the PHB as a consequence of intermolecular interactions that occur mainly in the amorphous regions of the two polymers. The interactions result in the formation of hydrogen bonding between the C=O groups of PHB and the hydroxyl groups of the straw, made widely available by the SEP.

The authors thank Dr. M. Rivola and Ms. M. Palma for their help in performing the FTIR experiments. The authors also thank “Progetto Finalizzato Chimica Fine II” of C.N.R. for supporting the application of a patent.

The work has been granted in the framework of an EC-ECLAIR project (AGRE CT 90 0044).

REFERENCES

1. D. Maldas, B. V. Kokta, and D. Dancault, *J. Appl. Polym. Sci.*, **37**, 751 (1989).
2. R. G. Raj, B. V. Kokta, D. Maldas, and D. Dancault, *J. Appl. Polym. Sci.*, **37**, 1089 (1989).
3. B. Focher, A. Marzetti, and V. Crescenzi, Eds., *Steam Explosion Techniques: Fundamentals and Applications*, Gordon and Breach Science Publs., Philadelphia, 1991.
4. R. H. Marchessault, S. Coulomba, H. Morikawa, and D. Robert, *Can. Chem.*, **60**, 2372 (1982).
5. M. Tanahashi, *J. Wood Res.*, **77**, 49 (1991).
6. R. P. Overend and E. Chornet, *Phil. Trans. R. Soc. Lond. A*, **321**, 523 (1987).
7. M. Lemoigne, *Ann. Inst. Past.*, **39**, 144 (1925).
8. P. J. Barham, A. Keller, E. L. Otun, and P. A. Holmes, *J. Mater. Sci.*, **19**, 2781 (1984).
9. M. Abbate, E. Martuscelli, G. Ragosta, and G. Scarinzi, *J. Mater. Sci.*, **26**, 1119 (1991).
10. T. P. Abbott, D. M. Palmer, S. H. Gordon, and M. O. Bayby, *J. Wood Chem. Technol.*, **8**, 1–28 (1988).
11. J. K. Kauppinen, D. J. Moffat, H. H. Mantsch, and D. Cameron, *Anal. Chem.*, **53**, 1454 (1981).
12. P. R. Griffiths, *Science*, **222**, 297 (1983).
13. G. R. Thomas Jr. and D. A. Agard, *Biophys. J.*, **46**, 753 (1984).
14. S. Bloembergen, D. A. Holden, G. K. Hamer, T. L. Bluhm, and R. H. Marchessault, *Macromolecules*, **19**, 2865 (1986).
15. L. Mandelken, *Crystallization of Polymers*, McGraw-Hill, New York, 1964.
16. A. J. Kinloch and R. J. Young, *Fracture Behaviour of Polymers*, Applied Science, London, 1983.
17. R. Greco and G. Ragosta, *J. Mater. Sci.*, **23**, 4171 (1988).
18. F. Coppola, R. Greco, and G. Ragosta, *J. Mater. Sci.*, **21**, 1775 (1986).

Received March 13, 1992

Accepted January 25, 1993